THE CONCRETE NZ CONFERENCE 2018
PROGRESS THROUGH COLLABORATION
Claudelands, Hamilton | 11 – 13 October 2018

RECTANGULAR RC WALLS UNDER BI-DIRECTIONAL LOADING: RECENT EXPERIMENTAL AND NUMERICAL FINDINGS

A. Niroomandi[1], S. Pampanin[2], R.P. Dhakal[2], M. Soleymani Ashtiani[3] and C. de la Torre[1]

[1] PhD candidate, Dept. of Civil and Natural Resources Engineering, University of Canterbury, Christchurch, New Zealand
[2] Professor, Dept. of Civil and Natural Resources Engineering, University of Canterbury, Christchurch, New Zealand; Dept. of Structural and Geotechnical Engineering, University of Roma" La Sapienza" Italy
[3] PhD, Structural Engineer, Ian Connor Consulting Ltd., Christchurch, New Zealand

ABSTRACT: Following the recent earthquakes in Chile (2010) and New Zealand (2010/2011), peculiar failure modes were observed in Reinforced Concrete (RC) walls. These observations have raised a global concern on the contribution of bi-directional loading to these failure mechanisms. One of the failure modes that could potentially result from bi-directional excitations is out-of-plane shear failure. In this paper an overview of the recent experimental and numerical findings regarding out-of-plane shear failure in RC walls are presented. The numerical study presents the Finite Element (FE) simulation of wall D5-6 from the Grand Chancellor Hotel that failed in shear in the out-of-plane direction in the February 2011 Christchurch earthquake. The main objective of the numerical study was to investigate the reasons for this failure mode. The experimental campaign includes the recent experiments conducted in the Structural Engineering Laboratory of the University of Canterbury. The experimental study included three rectangular slender RC walls designed based on NZS3101: 2006-A3 (2017) for three different ductility levels, namely: nominally ductile, limited ductile and ductile. The numerical results showed that high axial load combined with bi-directional loading caused the out-of-plane shear failure in wall D5-6 from the Grand Chancellor Hotel. This was also confirmed and further investigated in the experimental phase of the study.

1 Introduction

In the short but violent M_W6.2 Christchurch earthquake on 22 February 2011, the Grand Chancellor Hotel (GCH) building, located in the Central Building District, suffered major structural damage. In particular one of the main shear wall (wall D5-6) failed in a brittle manner at the ground floor level. The building had previously survived the 4 September 2010 and 26 December 2010 earthquakes without apparent significant structural damage and was fully operational when the February event occurred (Dunning Thornton 2011). The 22-storey GCH building was constructed in two phases. The lower 7 (or 14 half-height car park) storey structure, which comprises RC shear walls and cast-in-place flat slabs and columns, was constructed first in 1970s. The upper 15 full-height storey structure, which comprises of perimeter moment frames with a precast floor system, was added subsequently (Kam et al. 2011). The tower was constructed between 1985 and 1988 according to the NZS4203:1984 loading standard and NZS3101:1982 concrete design standard (Elwood 2013). Figure 1 shows the basic information regarding GCH building and wall D5-6 and its final failure. For

further details refer to studies conducted by Dunning Thornton Consultants Ltd (2011), Kam et al. (2011), Elwood et al. (2012) and Elwood (2013).
In this study, the mechanisms of the shear failure of the wall D5-6 in the out-of-plane direction was numerically investigated and further scrutinized through experiments in the laboratory.

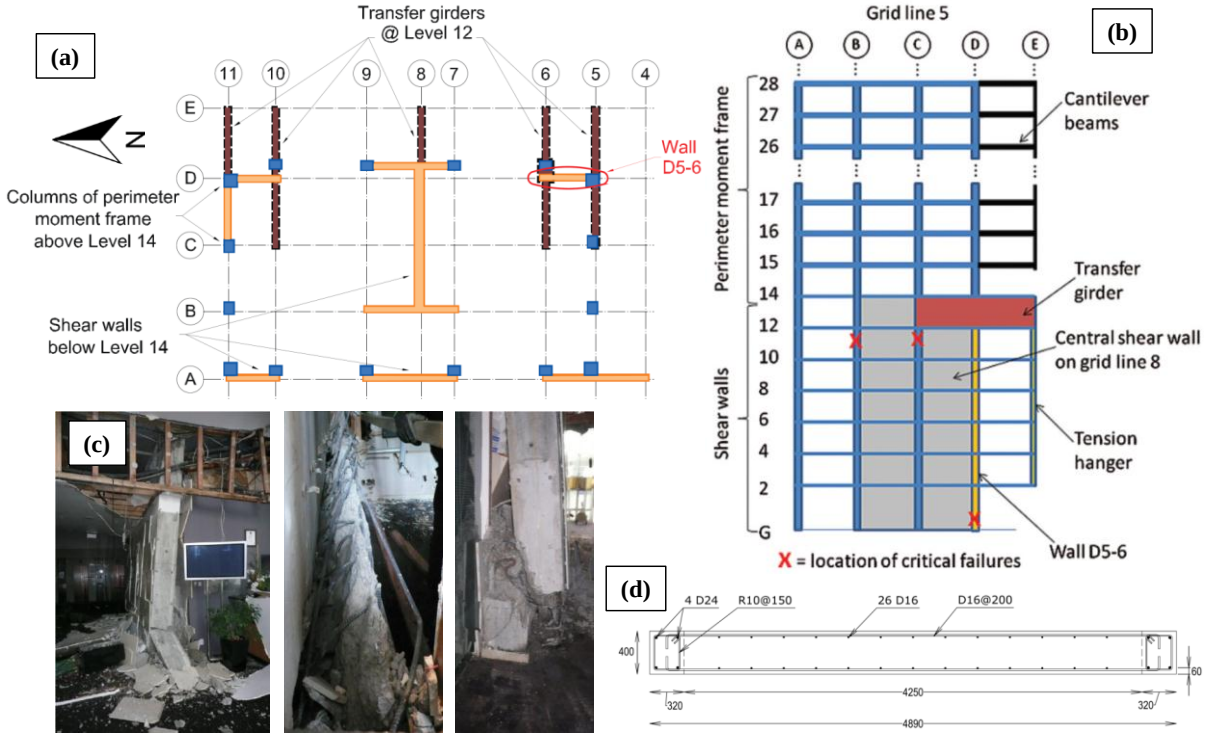

Figure 1 (a & b) GCH structural layout sketch plan and elevation along grid line 5 (Elwood 2013), (c) failure mode of wall D5-6 from GCH building in the 2011 NZ earthquake (Dunning Thornton 2011) and (d) details of the wall D 5-6 (Dunning Thornton 2011)

2 Directionally of the Canterbury's September 2010 and February 2011 earthquakes

It is known that ground motion intensity is not uniform in all orientations. In some cases ground motions can be polarized and the intensity in one orientation can be significantly stronger than in the other orientations (Campbell and Bozorgnia 2008, Huang et al. 2008). This phenomenon is often referred as "directionality" of ground motion. The locations of the four strong motion stations around Christchurch central business district that recorded the two earthquakes are shown in Figure 2 along with the location of GCH building. Figure 3 shows displacement responses for two Single Degree Of Freedom (SDOF) systems, representing the building's N-S (with T=2.4 sec) and E-W (with T=2.8 sec) orientations with 5% damping under the recorded ground accelerations from the 22 February 2011 and 4 September 2010 earthquakes at nearby strong motion stations shown in Figure 2. The responses from the two SDOF systems are plotted against each other to illustrate the directionality in the displacement response to these ground motions. The direction of the wall in regards to each earthquake is also shown in Figure 3. Figure 3 clearly illustrates north-south directionality in the displacement response at the fundamental period of the building to the 4 September 2010 earthquake, with most of the large displacement cycles oriented in this direction. On the contrary, the displacement response is more strongly directed to the east-west (i.e., the out-of-plane direction of the wall) under the 22 February 2011 earthquake. Similar conclusion regarding the direction of these earthquakes was also reported by Kam et al. (2011).

Figure 2 Locations of the 4 strong motion stations and the Grand Chancellor Hotel

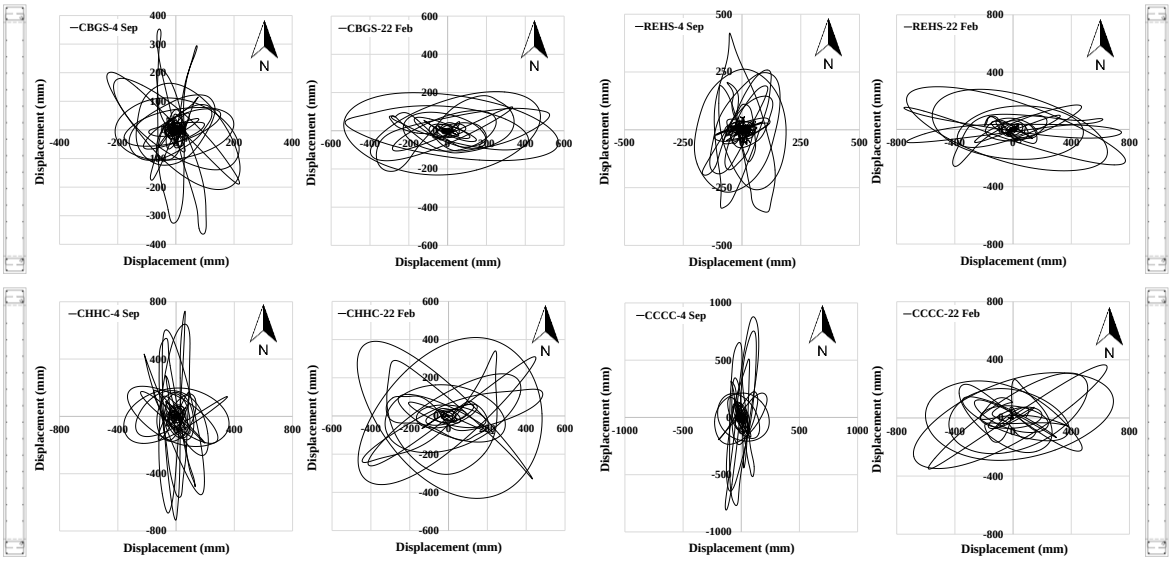

Figure 3 The directionality of ground motions from the 4 September 2010 and 22 February 2011 earthquakes recorded at four stations (i.e., CBGS, REHS, CHHC, and CCCC) is illustrated via orbit plots of displacement response which were created by plotting the displacement response of a SDOF element to the N-S component of ground motion versus the displacement response of a SDOF system to the E-W component of ground motion using periods of 2.4 and 2.8 seconds in the N-S and E-W directions, respectively, to represent the fundamental period of the structure in each respective orientation

3 Numerical simulation of the wall D5-6

The Finite Element (FE) software, DIANA (2015), was used to simulate the behaviour of the wall D5-6. Due to limitation with the number of pages for this paper, details of the FE model and its validation are not discussed here. For more information refer to Niroomandi et al. ((2016a), (2016b) and (2017)). In order to understand the effects of loading path on the seismic performance of wall D5-6, different loading regimes include in-plane uni-directional, out-of-plane uni-directional, skewed uni-directional and clover leaf bi-directional were applied to the wall. However, in this paper only the behaviour of the wall under in-plane uni-directional and out-of-plane uni-directional loading is discussed. Figure 4 shows the FE model of the wall under in-plane uni-directional and out-of-plane uni-directional loadings.

3.1 Base shear vs drift ratio

Figure 5 shows the base shear vs drift ratio as well as the failure point of the wall when it is under in-plane uni-directional (Figure 5a) and out-of-plane uni-directional loadings (Figure 5b). It was assumed that the wall had a cantilever deformation in the in-plane direction when it's under in-plane loading and a double bending deformation in the out-of-plane direction when it is under out-of-plane loading. Therefore, the in-plane shear span of the wall was

assumed 16375 mm (equal to the in-plane effective height of the wall) while the out-of-plane shear span of the wall was 2675mm (equal to half the height of the first storey). As can be seen in Figure 5b, the wall had a 42% strength reduction when out-of-plane shear failure occurred. This strength degradation of the wall when it was under out-of-plane loading was due to out-of-plane shear cracks which did not happen when the wall was under in-plane uni-directional loading only.

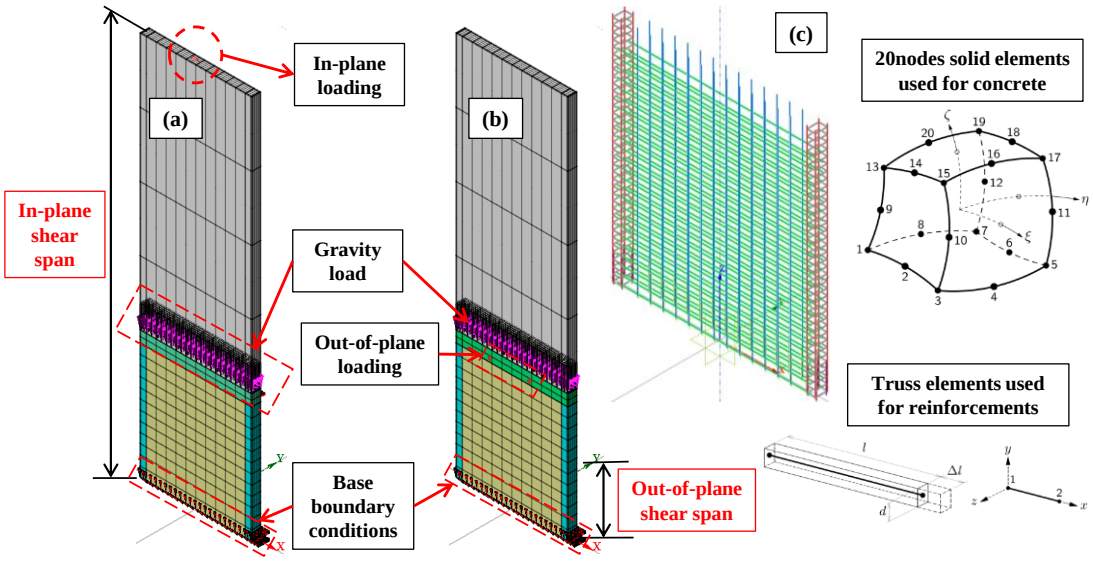

Figure 4 FE model of wall D5-6 in DIANA when under (a) in-plane uni-directional and (b) out-of-plane uni-directional loadings and (c) details of the reinforcements and elements used in the FE model

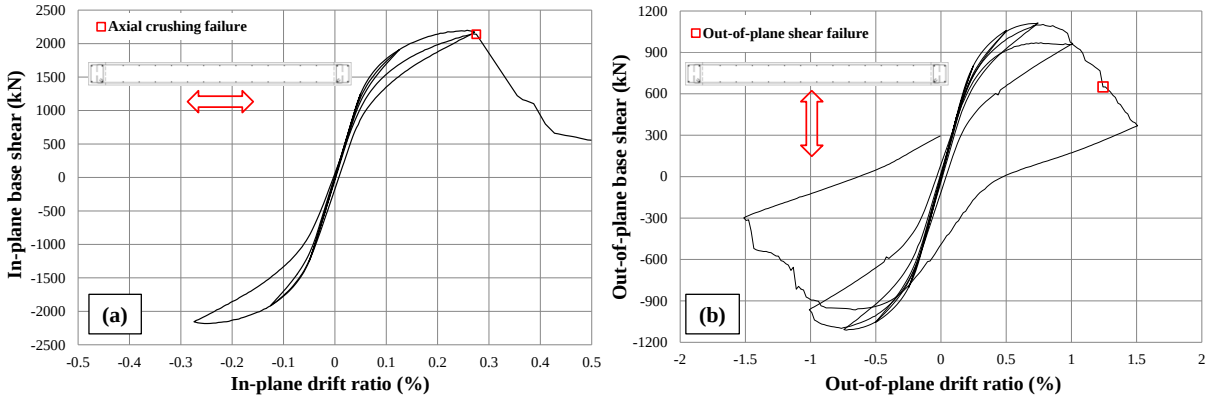

Figure 5 Base shear-drift ratio curve of wall D5-6 under (a) in-plane uni-directional and (b) out-of-plane uni-directional loadings

3.1.1 Failure mode of the wall D5-6 captured in DIANA

Figure 6 and Figure 7 show the behaviour of the wall under in-plane uni-directional loading before and after failure. As the axial strain and stress contours as well as the crack pattern show, the wall under in-plane loading failed in axial crushing resulted from high axial load and lack of confinement. It should be noted that in Figure 7, cracks are filtered to only show the major cracks and neglect the minor ones. However, when the wall was under out-of-plane loading, it failed in shear in the out-of-plane direction (Figure 8). Out-of-plane shear failure was defined as the point that out-of-plane shear cracks forms along the wall's length. Figure 9 compares the crack pattern resulted from FE analysis with the earthquake observations.

High axial load on the deformed wall acted as vertical shear along the wall and led to the out-of-plane shear failure of the wall. Low longitudinal reinforcement ratio and lack of sufficient out-of-plane ties were two of the important parameters that led to the final failure of the wall.

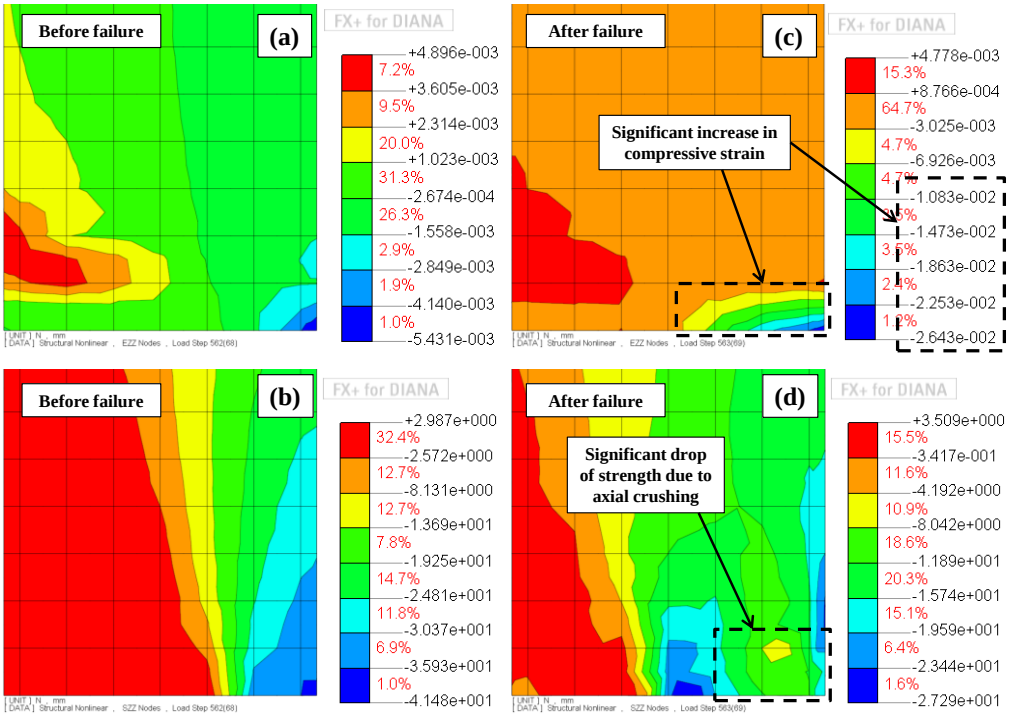

Figure 6 Wall D5-6 under in-plane uni-directional loading (a & b) axial strain and stress before failure, and (c & d) axial strain and stress after failure

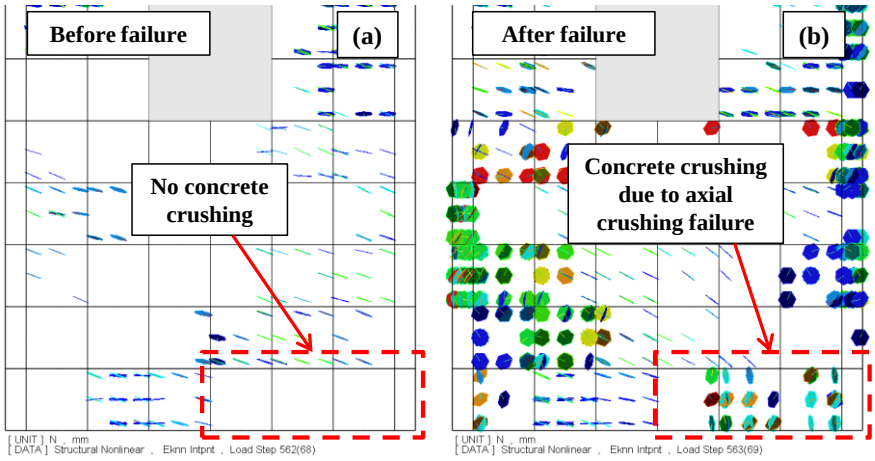

Figure 7 Crack pattern of Wall D5-6 under in-plane uni-directional loading (a) before and (b) after failure

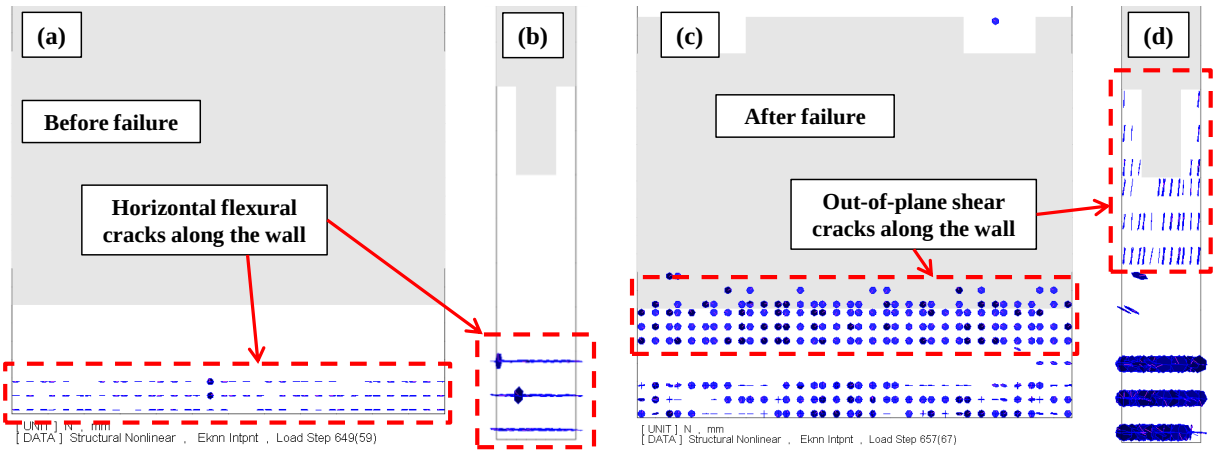

Figure 8 wall D5-6 under out-of-plane uni-directional loading (a & b) crack pattern before initiation of out-of-plane shear failure and (c & d) crack pattern after failure (both front and side views)

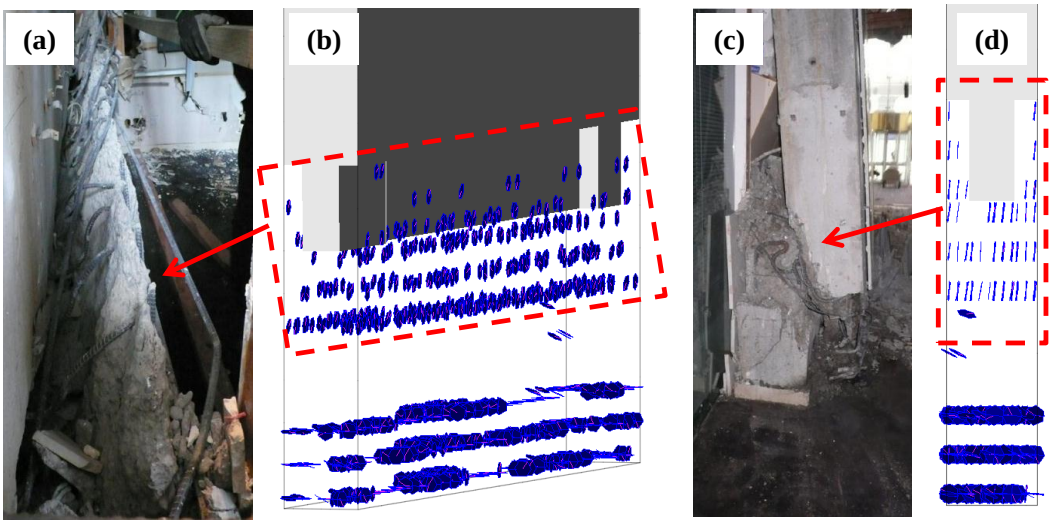

Figure 9 Crack pattern of wall D5-6 under out-of-plane uni-directional loading (a & c) February 2011 earthquake (Dunning Thornton 2011), (b & d) 3D and out-of-plane view of the cracks in DIANA

4 Experimental campaign

In order to further scrutinise the out-of-plane shear failure mechanism in RC walls, a series of experiments was conducted to first capture this failure mode in the laboratory and then further investigate its characteristics with the numerical model.

4.1 Experimental programme

The test series comprised of three rectangular RC walls designed for different ductility levels, namely nominally ductile, limited ductile and ductile based on NZS3101:3006-A3(2017). These walls were tested under a skewed uni-directional loading pattern. The two main reasons for choosing this loading pattern were:

1. In a series of tests by Niroomandi et al. (2018), out-of-plane shear cracks were only observed in the wall tested under skew loading (specimen SP1-Skew).
2. To simulate a loading pattern similar to the one imposed to wall D5-6 in the February 2011 Christchurch earthquake (discussed in Section 2).

4.1.1 Description of the test units

The specimens were 2:5 (40%) scale models of the first storey of a RC wall in a six-storey reference building with a total height of 21.43 m. The benchmark specimen (SP2-ND) was designed based on NZS3101:2006-A3 (2017) for a nominal ductility. SP2-ND was proved to be vulnerable to out-of-plane shear failure based on numerical results using DIANA (2015). The other two specimens namely, SP3-LD and SP4-D had the same geometry, axial load, total longitudinal and horizontal reinforcement ratios compared to SP2-ND. However, SP3-LD and SP4-D were designed for a limited ductile and ductile levels, respectively based on NZS3101:2006-A3 (2017). A quick summary of the test matrix is given in Table 1. Summary of the main geometrical features and reinforcement details are listed in Table 2. Cross-section and side-view of the reinforcement layout of SP2-ND is shown in Figure 10.

Table 1 Test matrix of the three RC walls specimens

Name	In-plane shear span ratio ($H_{e,inplane}/L_w$)	Out-of-plane shear span ratio (H_{out}/t)	Axial load ratio, $P/(A_g f'_c)$, using $f'_c = 30MPa$	Loading pattern	
				Type	Schematic view
SP2-ND	6000/1600 =3.75	2016/(160×2) =6.3	30%	Skewed uni-directional	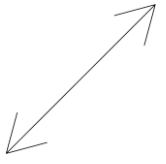
SP3-LD					
SP4-D					

Table 2 Details of the specimens

Specimen	SP2-ND	SP3-LD	SP4-D
Clear height, H_w (mm)	1650		
Length, L_w (mm)	1600		
Thickness, t (mm)	160		
Total longitudinal reinforcement ratio, $\rho_t = (A_{s,BZ} + A_{s,web}) / (L_w \times t)$	0.92%		
BZ transverse reinforcement ratio, $\rho_{sx} = A_{vx} / (s \times t)$	0.295%	0.739%	1.05%
BZ transverse reinforcement ratio, $\rho_{sy} = A_{vy} / (s \times l_{BZ})$	0.248%	0.53%	0.75%
Web transverse reinforcement ratio, $\rho_{s(web)} = A_{v(web)} / (s \times l_{web})$	-	-	0.326%
Web shear reinforcement ratio, $\rho_v = A_{sv} / (s \times t)$	0.655%		

4.1.2 Material properties

The average concrete compressive strength of the specimen SP2-ND on the test day was 27.6 MPa. The steel reinforcing bars used for the specimens were NZ Grade 300 and Grade 500 as indicated in Figure 10.

4.1.3 Test setup

A schematic view of the test setup used in this study to apply bi-directional loading is shown in Figure 11a. Seven hydraulic actuators were used to apply the gravity load and lateral in-plane and out-of-plane cyclic displacements. As only the bottom storey was tested, the effect of the higher stories was simulated by two in-plane 1000kN vertical actuators. Therefore the vertical actuators applied half of the gravity load and bending moment corresponding to the chosen in-plane shear span ratio through the actuators' lever arm. The third horizontal 1000kN actuator applied the lateral in-plane displacement to the specimen. Out of the four hydraulic actuators left, two horizontal 400kN actuators apply the out-of-plane cyclic displacements (identified as D in Figure 11) and two out-of-plane vertical 1000kN actuators were used to apply the second half of the axial load and to create a double bending deformation in the wall (identified as C in Figure 11). The double bending deformation shape in the out-of-plane represents the rigidity of the slab compared to the wall's stiffness in the out-of-plane direction. It should be noted that the wall had a cantilever deformation shape in the in-plane direction.

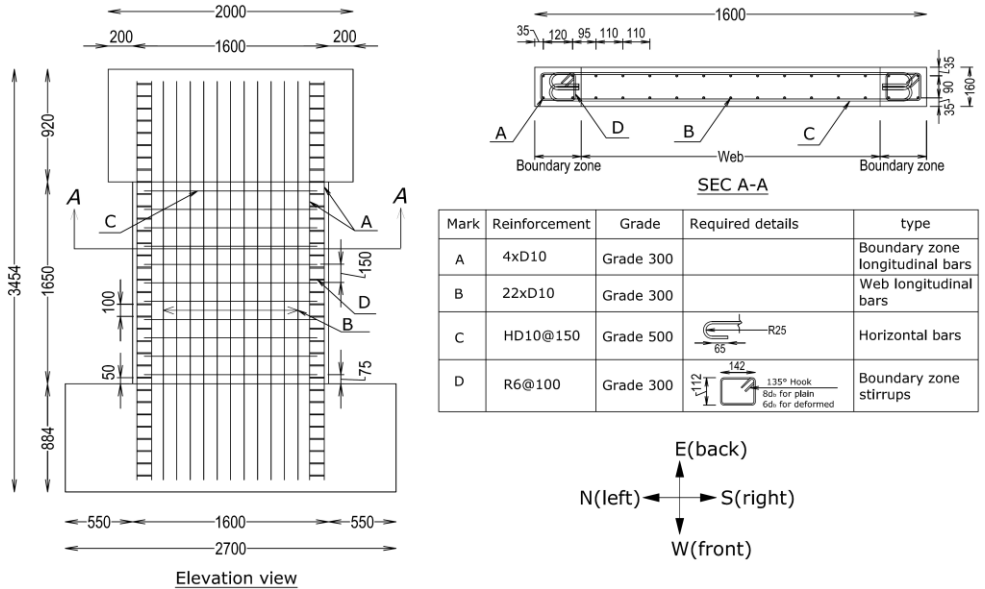

Figure 10 Details of the section and side view of the reinforcement layouts of the specimen SP2-ND

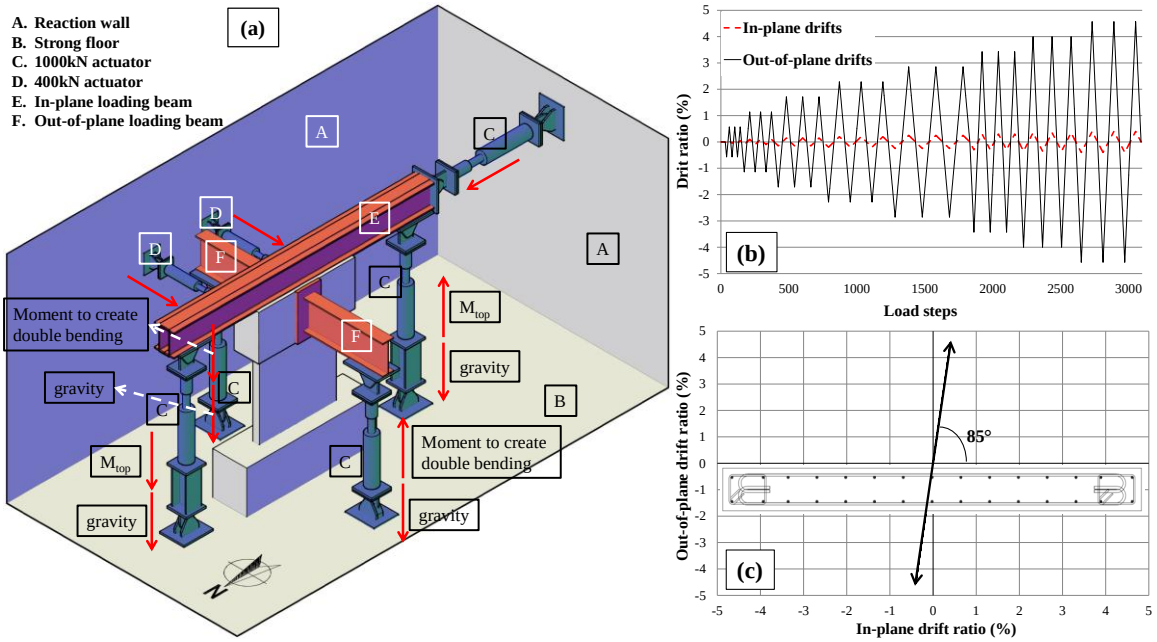

Figure 11 (a) schematic view of the test setup used for the specimens under bi-directional loadings and (b & c) loading protocol used for the experiment

4.1.4 Lateral Loading protocol

The loading protocol used in this study was a skewed uni-directional with a 85 degree angle with respect to the main in-plane axis which is shown in Figure 11b&c. The reasons for choosing this load path were discussed in Section 4.1. The lateral loading protocol used in this experiment in both in-plane and out-of-plane directions consisted of three displacement-controlled cycles at increasing amplitudes. These amplitudes are presented in Figure 11b and Table 3. In-plane and out-of-plane cyclic displacements were measured at a height of 2016mm.

Table 3 In-plane and out-of-plane drift ratios of each cycle

Cycle	1	2	3	4	5	6
In-plane drift ratio	0.05%	0.1%	0.15%	0.2%	0.25%	0.3%
Out-of-plane drift ratio	0.572%	1.143%	1.715%	2.286%	2.858%	3.429%

4.1.5 Instrumentation

All specimens were heavily instrumented using both conventional instruments and modern particle tracking measurement system. In addition, crack widths were measured at the peak drifts and photos were taken at the end of each displacement step. In order to make it easier when referring to each face of the specimen, as it is shown in Figure 10 and Figure 11, front face is the western, back face is eastern, right face is southern and left face is northern face of the specimen. Some of the instruments used are discussed briefly below.

Linear Variable Differential Transformer (LVDT): 23 vertical LVDTs on the front and 22 on the back faces of the wall used to measure average axial strain of concrete. On the back face, 6 diagonal LVDTs were used to capture the shear deformations of the wall.

Draw wire: On the back face, 16 draw wires were used to measure out-of-plane deformations of the wall. A draw wire was used to measure the in-plane deformations of the specimen.

Particle tracking: Further to these instruments, local deformations of the specimens were also measured on three faces of the specimen (front, left and right) using a Light Attenuation (LA) technique with Streams (Nokes 2016, Cenedese et al. 2017), a software tool developed at the University of Canterbury to support the analysis of images obtained from the experiment. For this purpose, random dots were painted on three faces of the specimen for particle tracking (see Figure 12-Figure 15).

4.2 Test observations of SP2-ND

In this paper, only the experimental results of the benchmark specimen (SP2-ND) were reported. As was discussed, this specimen was designed for a nominal ductility based on NZS3101:2006-A3 (2017) and was expected to be prone to out-of-plane shear failure based on numerical results.

The first sign of cover concrete spalling was observed in the left side from the second cycle of 0.05% in-plane and 0.57% out-of-plane drift ratios. However, there was no sign of vertical splitting in the right side during this drift level. Horizontal tensile cracks on the front and back sides formed along the wall at a height of about 100mm above the base with a length of 1400 and 1100 mm, respectively. Maximum crack width by the end of 0.05% in-plane and 0.57% out-of-plane drift ratios was 0.2mm. There was no sign of residual cracks during this drift level. Vertical splitting in concrete cover increased in the left side and initiated in the right side from the first cycle of 0.1% in-plane and 1.14% out-of-plane drift ratios and penetrated the boundary zone and web (Figure 12). Horizontal tensile cracks formed along the full length of the wall at a height of about 100mm on the front side with a maximum crack width of 0.8mm. On the back face, horizontal tensile cracks formed along the wall with a length of about 1400 mm with a maximum crack width of 0.8 mm. Maximum residual crack width was 0.25 mm during this drift level.

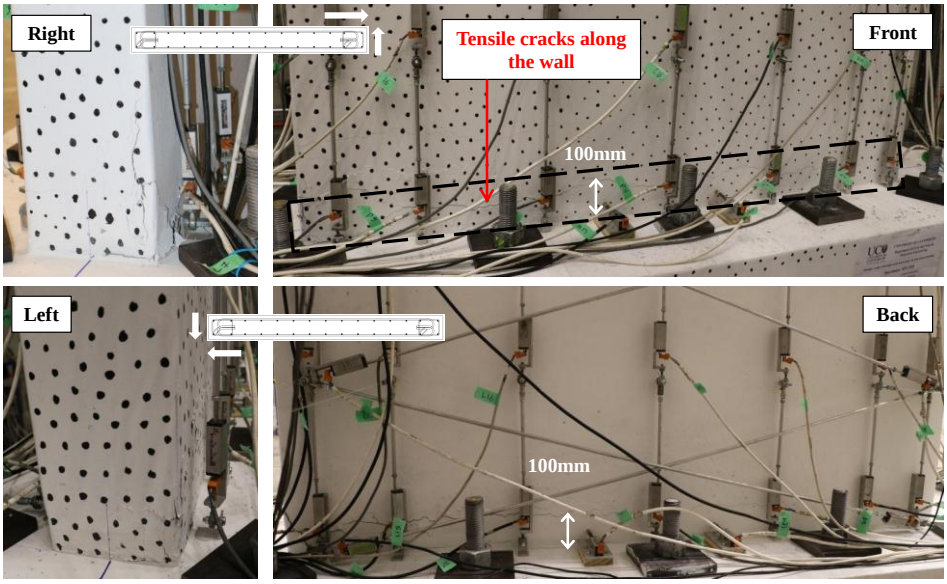

Figure 12 Specimen SP2-ND at 0.1% in-plane and 1.14% out-of-plane drift ratios

The first sign of out-of-plane shear cracks was observed from the first cycle of 0.15% in-plane and 1.72% out-of-plane drift ratios (Figure 13). During this drift level, the maximum crack width increased significantly to about 3mm. The maximum residual crack width was about 0.8-1mm by the end of 0.15% in-plane and 1.72% out-of-plane drift ratios.

The specimen failed suddenly while applying the first cycle of 0.2% in-plane and 2.29% out-of-plane drift ratios half way through that cycle. Figure 14 shows the specimen just before and after the failure.

Description of the failure mechanism

Out-of-plane shear cracks initiated from the first cycle of 0.15% in-plane and 1.72% out-of-plane drift ratios in both left and right sides and developed by the end of the third cycle of this drift level (Figure 13). Consequently the specimen failed in an extremely brittle manner during the first cycle of 0.2% in-plane and 2.29% out-of-plane drift ratios, half way through the first cycle (Figure 14). Failure of the specimen involved a diagonal sliding of about 23mm transverse to the wall from its left side, penetrating almost along the full length of the wall (Figure 15). A lateral deformation of about 23mm was observed in the right hand side of the wall on a length of about 150mm (Figure 15). There was no sign of bar buckling before the

out-of-plane shear failure. However, as can also be seen in Figure 15, all the longitudinal bars along the wall buckled after the failure. Buckling of the longitudinal bars could have been turned into a bar rupture along the wall if the amount of longitudinal bars was less, similar to what happened to the Grand Chancellor Hotel's wall D5-6 (Figure 1). It is worth noting that the longitudinal reinforcement ratio of the specimen SP2-ND was 0.92% while it was 0.452% in the case of wall D5-6. In accordance to what was observed in the numerical study, high axial load on the deformed wall acted as vertical shear along the wall and sheared off the wall while the wall lacked sufficient out-of-plane ties.

Base shear vs drift ratio of the wall

Figure 16 shows the base shear vs drift ratio of the specimen SP2-ND in the in-plane and out-of-plane directions. Initiation of concrete cover spalling, out-of-plane shear failure and final failure point are shown in Figure 16. Initiation of out-of-plane shear failure was considered when shear cracks formed transverse to the wall (see Figure 13). The specimen had 33% out-of-plane strength reduction from its left side and 46% from its right face before failure.

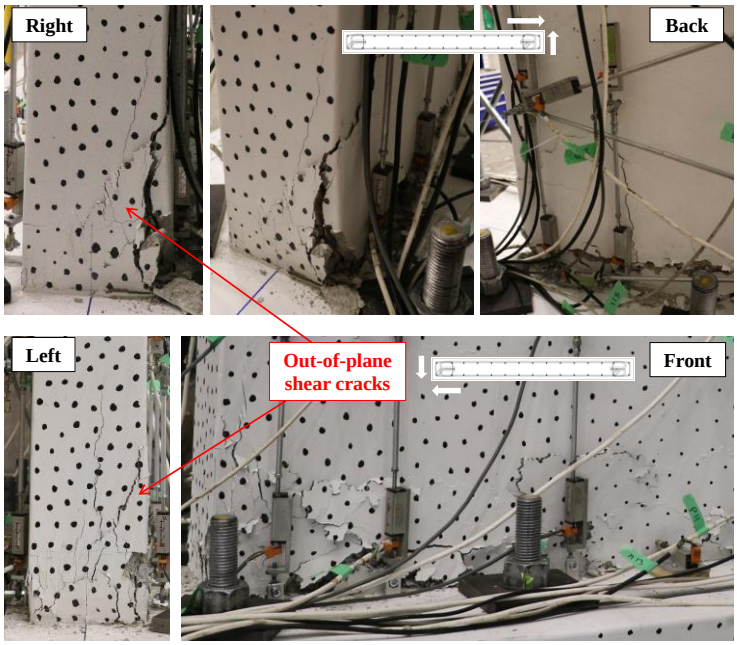

Figure 13 Specimen SP2-ND at 0.15% in-plane and 1.72% out-of-plane drift ratios

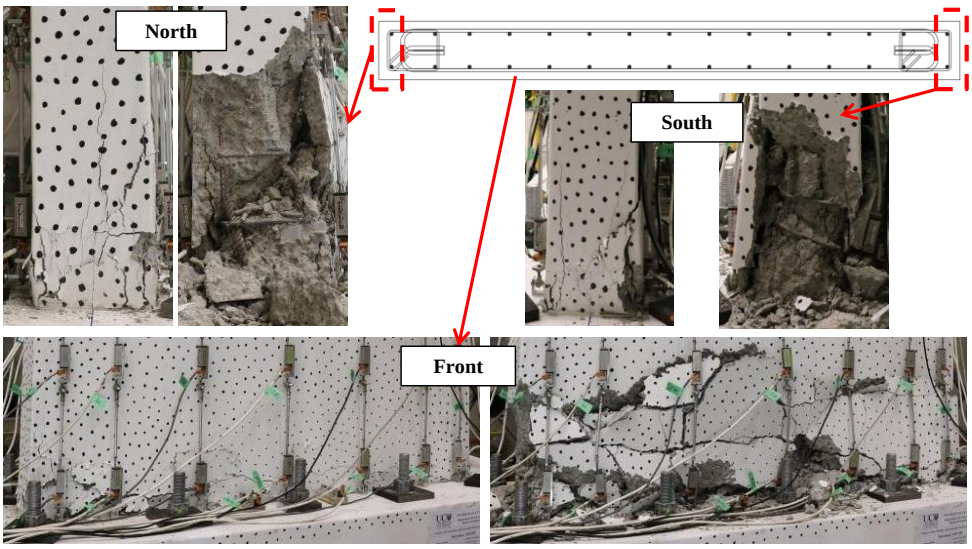

Figure 14 Specimen SP2-ND just before and after out-of-plane shear failure

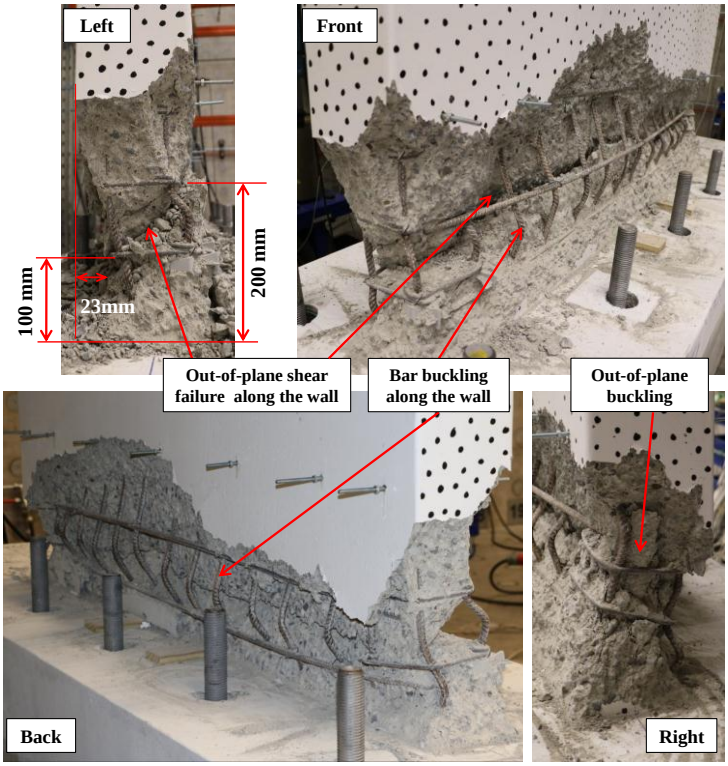

Figure 15 SP2-ND failure mode after removing the concrete spalling pieces

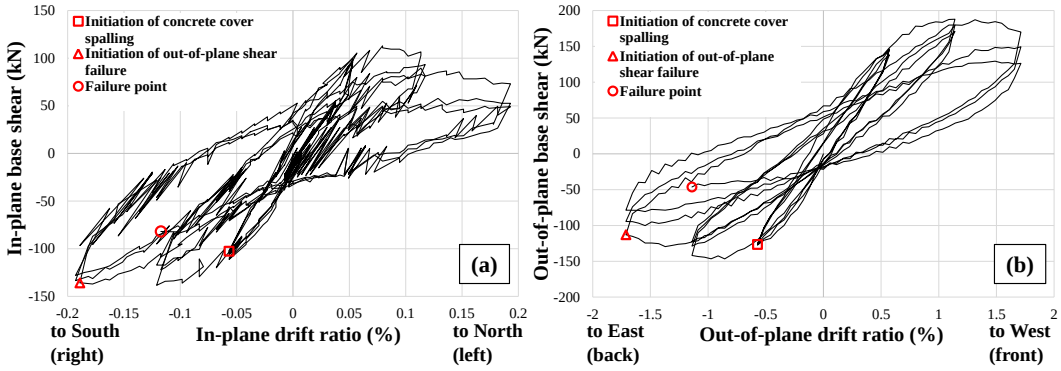

Figure 16 Base shear - drift ratio of SP2-ND in the (a) in-plane and (b) out-of-plane directions

5 Conclusions

This paper presents an overview of the results of the study on the failure mode observed in the wall D5-6 from the Grand Chancellor Hotel in the 22 February 2011 Christchurch earthquake. The main aspect that was investigated by means of this study concerns the reasons behind the failure mode observed in the wall. The numerical as well as experimental findings of this study are summarised below:

- The displacement response of SDOF oscillators at the fundamental period of the building in each direction from the 4 September 2010 earthquake is strongly oriented in the in-plane direction, while the response from the 22 February 2011 earthquake was strongly in the out-of-plane direction of the wall D5-6 from Grand Chancellor Hotel.
- The FE analysis of the wall D5-6 under uni-directional loading in the in-plane and out-of-plane directions showed that the bi-directional loading can change the failure mode of the wall from an axial crushing to a shear failure in the out-of-plane direction.
- The experimental study conducted on a RC wall with similar characteristics to wall D5-6 from the Grand Chancellor Hotel showed similar failure mode to what observed in the Christchurch 2011 earthquake. The failure mode observed in the experiment was

extremely sudden and unexpected, involving a diagonal sliding transverse to the wall, penetrating certain length of the wall accompanied by buckling of longitudinal bars along the wall.

- The full rupture observed in wall D5-6 was not observed in the experiment since the longitudinal reinforcement ratio of the specimen SP2-ND was double the case of wall D5-6.
- The numerical as well as experimental results showed that high axial load acts as vertical shear on a wall with out-of-plane deformation and shears off the wall when it lacks enough shear capacity.

6 References

Campbell, K. W. and Y. Bozorgnia (2008). "NGA ground motion model for the geometric mean horizontal component of PGA, PGV, PGD and 5% damped linear elastic response spectra for periods ranging from 0.01 to 10 s." *Earthquake Spectra* 24(1), 139-171.

Cenedese, C., R. Nokes and J. Hyatt (2017). "Lock-exchange gravity currents over rough bottoms." *Environmental Fluid Mechanics*, 1-15.

DIANA (2015). DIANA Manual Release 9.6, TNO DIANA BV. Delft, the Netherlands.

Dunning Thornton (2011). Report on the structural performance of the Hotel Grand Chancellor in the earthquake on 22 February 2011. A report to the Department of Building and Housing (DBH), Dunning Thornton Consultants Ltd., Wellington, New Zealand.

Elwood, K., S. Pampanin and W. Y. Kam (2012). 22 February 2011 Christchurch earthquake and implications for the design of concrete structures. *Proc., The International Symposium on Engineering Lessons Learned from the 2011 Great East Japan Earthquake*, Tokyo, Japan.

Elwood, K. J. (2013). "Performance of concrete buildings in the 22 February 2011 Christchurch earthquake and implications for Canadian codes." *Canadian Journal of Civil Engineering* 40(3), 759-776.

Huang, Y.-N., A. S. Whittaker and N. Luco (2008). "Maximum spectral demands in the near-fault region." *Earthquake Spectra* 24(1), 319-341.

Kam, W. Y., S. Pampanin and K. J. Elwood (2011). "Seismic performance of reinforced concrete buildings in the 22 February Christchurch (Lyttelton) earthquake." *Bulletin of the New Zealand Society for Earthquake Engineering* 44(4), 239-278.

Niroomandi, A., S. Pampanin, R. P. Dhakal and M. Soleymani Ashtiani (2016a). Finite element analysis of RC rectangular shear walls under bi-directional loading. *Proc., The New Zealand Society for Earthquake Engineering (NZSEE) Annual Technical Conference*, Christchurch, New Zealand.

Niroomandi, A., S. Pampanin, R. P. Dhakal and M. Soleymani Ashtiani (2016b). Finite element analysis of rectangular reinforced concrete walls under bi-directional loading. *Proc., The New Zealand concrete industry conference*, Auckland, New Zealand.

Niroomandi, A., S. Pampanin, R. P. Dhakal and M. Soleymani Ashtiani (2018). Experimental study on slender rectangular RC walls under bi-directional loading. *Proc., Eleventh U.S. National Conference on Earthquake Engineering*, Los Angeles, California.

Niroomandi, A., M. Soleymani Ashtiani, S. Pampanin and R. P. Dhakal (2017). Numerical Investigations on Rectangular Squat Reinforced Concrete Walls under Bi-Directional Loading. *Proc., 16th World Conference on Earthquake Engineering*, Santiago Chile.

Nokes, R. (2016). Streams 2.05—system theory and design. University of Canterbury, Christchurch.

NZS3101:2006-A3 (2017). Code of Practice for the Design of Concrete Structures, Standards Association of New Zealand.